ICOCEM
4. International Conference on Civil and Environmental Geology and Mining Engineering
Trabzon - TURKEY
20 - 22 APRIL 2019

Lithologic Mapping and 2D-Geoelectrical Tomographic Delineation of Graphite Deposit within Kagara, part of Tegina Sheet 142, North-Central Nigeria

Christopher Imoukhai UNUEVHO[1*], A. Nnosike AMADI[1], L. Olarewaju ABDULAMEEN[1], E. Oluwatobi ADEGOKE[1], S. Jude EJEPU[1], E. Emeka UDENSI[2]

[1] Department of Geology, Federal University of Technology, Minna, Nigeria
[2]Department of Physics, Federal University of Technology, Minna, Nigeria

*Corresponding Author: unuevho@gmail.com

Abstract

Lithologic mapping, 1D geo-electrical sounding and 2D geo-electrical tomography were conducted to delineate graphite deposits in Kagara, North-Central Nigeria. The United States of America and European Union recently included Graphite among the minerals in critical global supply. Yet no attention has hitherto been given to ascertaining subsurface continuity of Kagara graphite outcrops, and their spatial extent has remained unknown. Outcrops found during the lithologic mapping are schist, amphibolite, quartzite and granite. The graphite outcrops are in sharp lateral contact with the quartzite outcrops. The geoelectrical data were acquired with ABEM Terrameter (SAS 4000). Schlumberger array was employed to conduct 1D resistivity, spontaneous potential (SP) and induced polarization (IP) sounding along a traverse aligned in outcrops' strike direction in order to characterise the graphite deposits electrically. Werner Alpha array was employed to acquire 2D geoelectrical data along outcrop strike and dip directions in order to verify the 1D geoelectrical characterization, and to ascertain subsurface continuation of the deposit. The 2D data were processed and interpreted using RES2DINV computer program. The geoelectrical data revealed that the graphite deposits' resistivity, IP and thickness respectively range from 2.4 - 93.3 Ωm, 2.5 -120 ms, and 8.1-11.3 m. The data also revealed that graphite outcrops are continuous in the subsurface along outcrops' strike and dip directions. The spatial extent of the graphite deposits was delineated within other lithologic outcrops, using the graphite outcrops' spatial locations and their inferred subsurface extension. The spatial extent of the deposit was estimated to be 1470509.0 m^2. This and its average thickness of 10.0 m give the graphite deposit an estimated gross volume of 14705090.0 m^3. Employment and additional revenue would be generated by Nigerian government from the development of the deposits and other graphite deposits in the country.

Keywords: Critical global supply, Graphite deposit, Geolectric characterization

Introduction

Natural graphite combines high thermal stability with high electrical conductivity (or very low electrical resistivity), chemical inertness, compressibility, elasticity and lubricity (Anthony, 2003; Wissler, 2006). This combination of physical properties makes graphite an irreplaceable material in manufacturing batteries, refractory, lubricants, brake linings and foundries (Shaw, 2013). It is the commonest anode material in Li-ion batteries utilised in driving electric and hybrid electric vehicles, and in large-scale electric storage devices such as cellular phones, laptops and super capacitors (Yoo et al., 2014; Dickson, 2014; Simandl et al., 2015). These utilities of graphite have so spiked upwards its demand that the United States and European Union recently declared it a mineral in critical global supply. Small graphite deposits previously considered economically unattractive now upgrade to ore status (Meunier, 2015). This is a window of opportunity for Nigeria to broaden her revenue source.

In spite of the critical global demand for graphite, the graphite outcrops in Kagara mentioned in Ajibade et al. (2008) have neither been spatially delineated nor quantitatively estimated. Both exercises are requirements for developing the deposit to create jobs and generate revenue.

Chernicoff and Whitney (2007) described identification of rocks in hand specimen. They employed mafic mineral index and texture to identify granites, granodiorites, diorites, gabbros, peridotites, rhyolite, dacite, and basalts. They also employed mineral content, mineral grain size and type of mineral foliation to identify slate, phyllite, schist, gneiss and amphibolites in hand specimens. Simandl et al. (2015) described graphite as a low density and high electrically conductive , opaque, gray-black, soft (1-2 on Mohr hardness scale) substance with greasy feel and dark gray streak. Robinson et al. (2017) remarked that graphite occurs within supercrustal metasedimentary belts wherein protolith organic-rich shale underwent metamorphism and concomitant graphitization within plate convergence zones. The heat and pressure for the metamorphism and graphitization of the organic-rich sediment are generated from the tectonomagmatic activity at the plate convergence zone. They continued that outcrop examination is an essential aspect of prospecting for graphite because graphite's chemical inertness makes it resistant to weathering and distinctly identifiable in outcrops. They also stated that promising subsurface graphite targets can be delineated by methods that measure spatial variation in electrical resistivity, because of graphite's high electrical conductivity. Scott (2014) prepared a geophysical manual on mineral prospecting for Newfoundland and Labrador Department of Natural Resources. He stressed that geophysical methods measure physical property of rocks, in order to delineate areas with anomalous values that coincide with spatial variation in geology and targets of economic interest. He further stressed that graphite bodies are characterised by low electrical resistivity and high electrical polarization.

Gandhi et al. (2016) distinguished between the morphology of mineral deposits. They described mineral deposits that are elongated in two directions compared to the third direction as flat bodies of mineral deposits. They identified sheet mineral bodies as flat bodies of mineral deposits that are separated from surrounding rocks by planar stratigraphic contacts. They also identified vein mineral bodies as mineral accumulations within fracture cavities, or mineral accumulations resulting from metasomatic replacement of rocks bodies along cracks.

They described mineral bodies that taper out markedly in all directions as lensoid or lenticular mineral accumulation.

Kagara is located within latitude N10°10'30" to N10°11'55" and longitude E6°14' 30" to E6°16' 0" (Figure 1) on Nigeria's Tegina Sheet 142 topograhic map. This lies within northern Nigerian Basement Complex (Figure 1), where it constitutes part of the Birnin Gwari Schist belt.

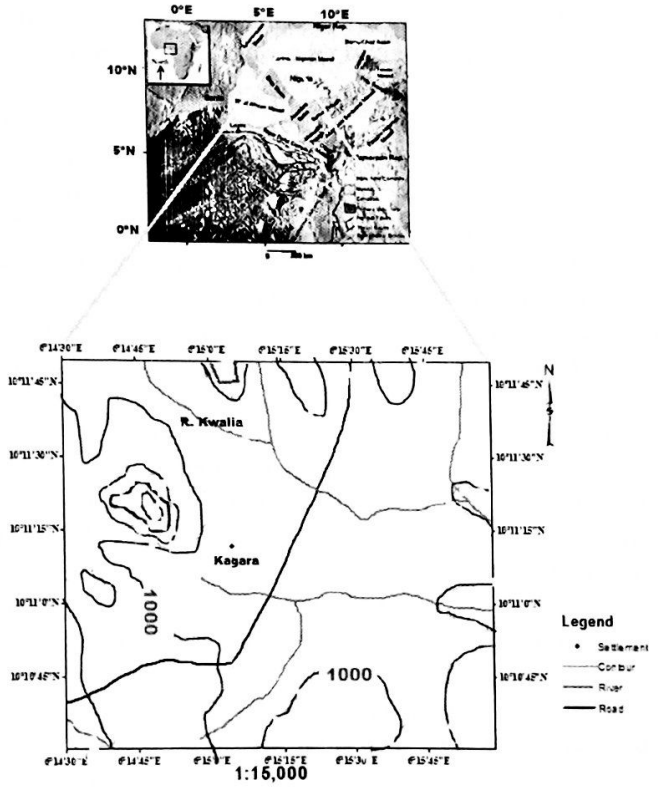

Figure 1.Study Areas

Material and Method

Base map for the surface lithologic mapping was prepared on a scale of 1: 15000 from Tegina Sheet 142 topographic map of Nigeria. Identification of igneous rocks in hand specimen was conducted using texture and Mafic Colour Index (MCI), which is the percentage of visible mafic (green, dark gray, black) minerals in the rock. Rocks with 0-15% were regarded as felsic. Felsic rocks in which potassium feldspar (pale orange to pink coloured) is greater than plagioclase feldspar (light gray coloured) were named granites. Mineral content and grain size were combined with presence or absence of gneissic and schistose mineral foliation to identify metamorphic rocks in hand specimen. Quartzite was identified as non-foliated rocks constituted by quartz minerals that are fused together. Heavy rocks containing medium-coarse grained glossy black crystals with cleavages meeting at about 60°/ 120° were named amphibolites. Rocks that contain visible light gray to gray minerals, which split along unidirectional parallel planes, were called schists. Graphite exposures were identified using their low weight, opaque nature, gray-black colour, hardness of 1-2 on Mohr hardness scale,

greasy feel and dark gray streak. 1D geoelectric data, as well as continuous vertical electrical sounding (also known as electrical tomography or 2D geolectrical surveying) data, were used to characterize the graphite bodies electrically. ABEM Terrameter (SAS 4000) was employed in the geoelectrical data acquisition. 1D resistivity, induced polarization (IP) and spontaneous potential (SP) sounding were conducted in the vicinity (about 0.30 m offset distance) of a graphite outcrop. The Schlumberger field geometry was employed with acquisition electrodes arrayed along a 200 m traverse in the outcrop strike (N-S) direction. The 1D resistivity sounding data was processed and interpreted using WinRESIST version 1.0 for 1D resistivity data inversion. The measured one dimensional IP and SP values were plotted against electrode spacing using Micosoft Excel. Discontinuities were related to subsurface intervals of overburden, graphite bodies and fresh basement. The 2D geoelectrical data for characterizing the graphite bodies was acquired using the Werner Alpha geometry with sixteen electrodes arrayed along 30 m traverse in the strike of the outcrops. The minimum electrode spacing for the measurement was 2 m. The spacing was consecutively expanded in multiples of 2, 3, 4 and 5, thereby giving six data levels and a total of 35 data points.

Two 2D geoelectrical resistivity and induced polarization surveying were also conducted between the graphite and other rock outcrops, along 200 m overburden covered traverse in outcrop dip direction. This was to ascertain subsurface continuity of the graphite bodies because lithologic units do change along dip direction. The survey employed 21 electrodes, and 5 m minimum electrode spacing which was expanded consecutively in multiples of 2, 3, 4 and 5 to give 6 levels of measurement and 63 data points.

The 2D geoelectrical data were processed and interpreted using RES2DINV computer program. Keary et al (2002), Milson (2003) and Reynolds (2011) gave the resistivity values of weathered bedrock (overburden), graphite bodies, schist and quartzite as 100-1000 Ωm, 10-100 Ωm, 50-1000 Ωm and 100-200000 Ωm respectively. These values guided identification of overburden interval and graphite bodies. Inferred subsurface graphite bodies were combined with the graphite outcrop locations to delineate spatial extent of the graphite deposits within lithologic outcrop map. The area of the delineated spatial extent was estimated manually. The gross volume of the graphite body was estimated as product of the average its thickness and area.

Research Findings and Discussion

Outcrops of schist, quartzite, amphibolites and graphite bodies were found during the surface lithologic mapping. The schist, amphibolites and graphite bodies generally strike NNW-SSE (352°) and dip 25°westwards. The schists are micaceous and quartzose (Figures 2 and3), and graphitic (Figures 4 and 5).

Figure 2. Micaceous and quartzose schist

(6°15'15 "E, 10°10' 45 "N)

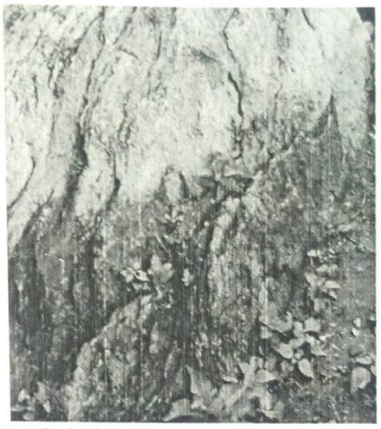

Figure 3. Micaceous and quartzose schist
(6°15'37 "E, 10°11'07 "N)

Figure 4. Graphitic schist (6°15'40.80 "E, 10°11'18.12"N)

Figure 5. Graphitic schist (6°15'46.08 "E, 10°11'33.62 "N)

Figures 6 and 7 are outcrops of quartzite bodies .

Figure 6. Quartzite outcrop (6°15'39.44"E, 10°11'22.31"N)

Figure 7. Quartzite outcrop
(6°15'40.79"E, 10°11'18.14 ' 'N)

Figures 8 and 9 are outcrops of amphibolites.

Figure 8. Amphibolite outcrop (6°15'53.72"E, 10°11'44.11 ' 'N)

Figure 9. Amphibolite outcrop (6°15'48.35"E, 10°11'16.11 ' 'N)

Some of the granitic outcrops are Figures 10 and 11. They carry xenoliths of schist, which indicates that the granitic bodies intruded into the schist.

Figure 10. Amphibolite outcrop (6°15'43.13"E, 10°11'0.3' 'N)

Figure 11. Amphibolite outcrop (6°15'20.14"E, 10°10'20.14 ' 'N)

Figures 12 and 13 are outcrops of graphite bodies.

Figure 12. Graphite outcrop (6°15'46.08"E, 10°11'36.62 ' 'N)

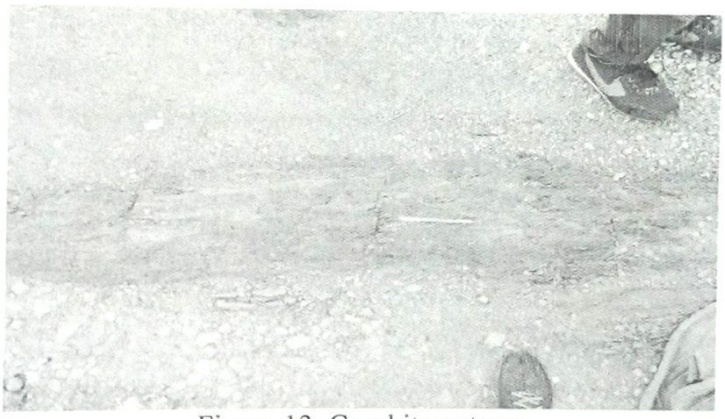

Figure 13. Graphite outcrop
(6°15'40.27"E, 10°11'22.39 ' 'N)

Figure 14 is the spatial locations of the outcrops of the lithologic units.

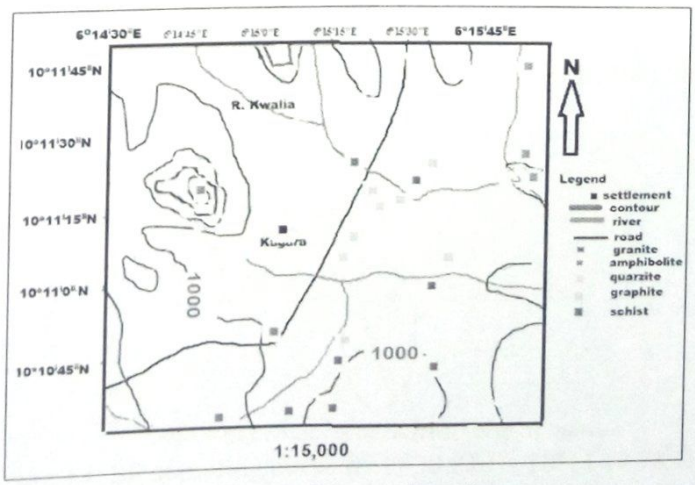

Figure 14. Outcrop locations

The locations of the 1D geoelectric sounding and 2D geoelectric surveys as well as outcrops are shown Figure 15.

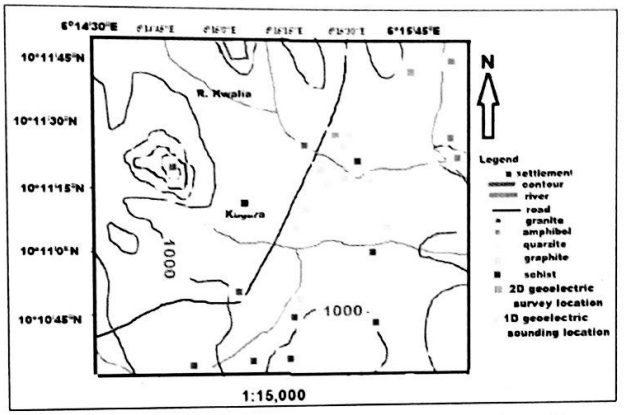

Figure 15. Geoelectric survey and outcrop locations

Figures 16, 17 and 18 are respectively the results of 1D resistivity, SP and IP sounding conducted (at Longitude 6°15'30.22"E and Latitude 10°11'40.78"N) in the vicinity of a graphite outcrop.

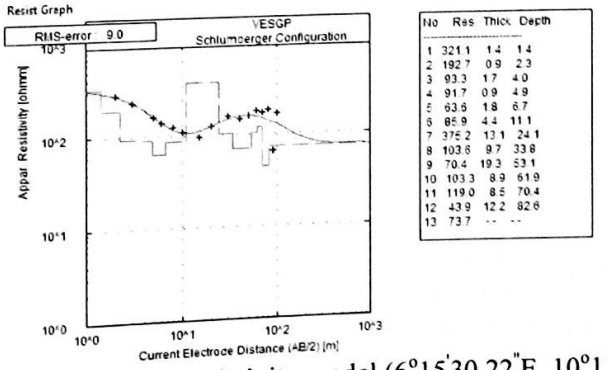

Figure 16. 1D subsurface resistivity model (6°15'30.22"E, 10°11'40.78"N)

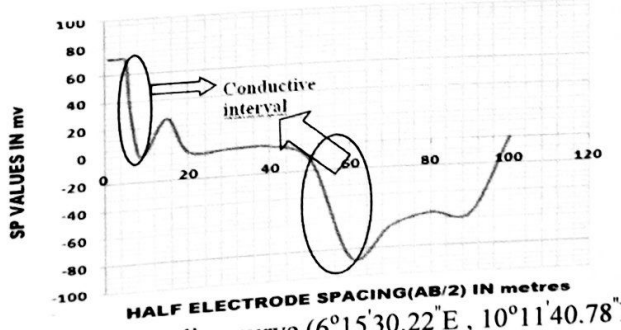

Figure 17. SP sounding curve (6°15'30.22"E , 10°11'40.78"N)

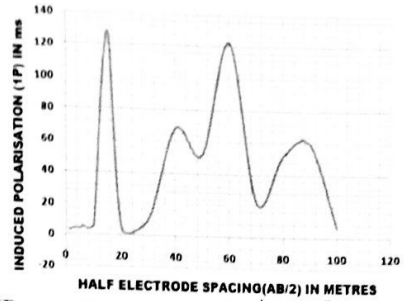

Figure 18. IP sounding curve (6°15'30.22"E , 10°11'40.78"N)

The 1D subsurface resistivity model (Figure 16) presents resistivity values of 93.3 to 63.6 Ωm between 3.0 – 11.1m depth. This reflects a continuous graphite body within the depth interval. The drop in SP values from 72.0 to -0.2 mv within this depth interval supports the presence of a continuous conductive body observed to be graphite on the surface. The IP values range from 4 - 120 ms in the depth interval. Low electrical resistivity and high chargeablity do mark graphite bodies (Scott, 2015).

Figures 19 and 20 are respectively 2D subsurface chargeability (IP) and resistivity models employed with the 1D geoelectric information to characterise the graphite body geoelectrically.

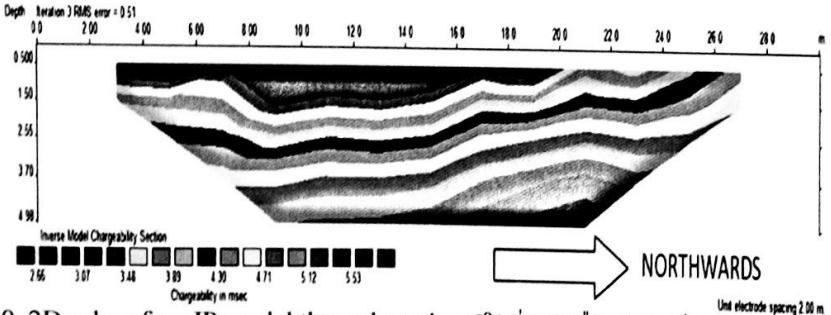

Figure 19. 2D subsurface IP model through station 6°15'30.22"E; 10°11'40.78"N, along strike (N-S traverse)

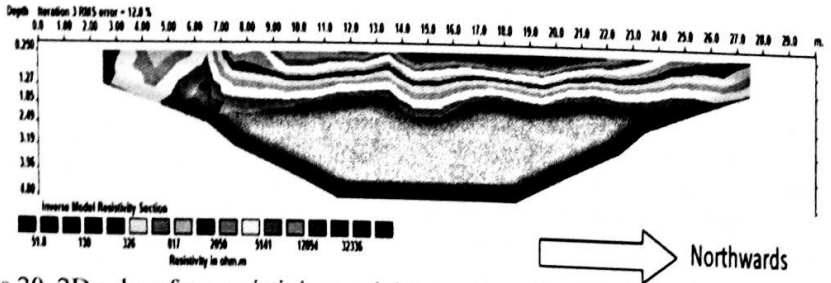

Figure 20. 2D subsurface resistivity model through station 6°15'30.22"E; 10°11'40.78"N, along strike (N-S traverse)

The 2D models show parallel subsurface geoelectric layers aligned northwards, which confirms that the acquisition traverse was along strike. The 1D geoelectric sounding station coincides with 14 m mid-electrode position on the 2D models. At this position, chargeability increases (from 3.0 to 5.0 ms) and resistivity decreases (from 320.0 to50 Ωm) within 2.2 to 4.50 m depth interval on the 2D models. This is the interval occupied by the subsurface graphite body. Figures 21 and 22 are 2D subsurface resistivity and IP models obtained from 2D geoelectrical traverse across strike (East-West) at the 1D sounding station.

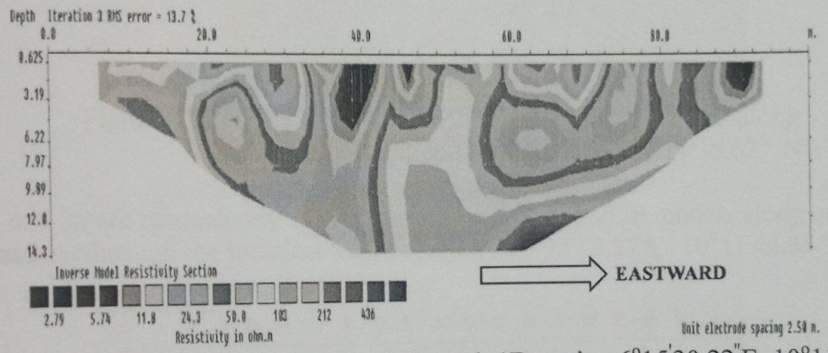

Figure 21. 2D subsurface resistivity model through 1D station 6°15'30.22"E; 10°11'40.78"N, across outcrop strike (E-W or dip direction traverse)

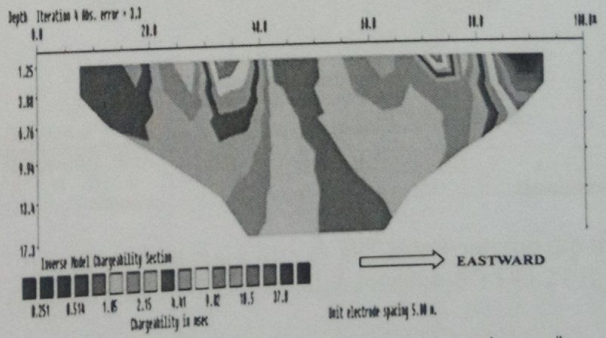

Figure 22. 2D subsurface IP model through 1D station 6°15'30.22"E; 10°11'40.78"N, across outcrop strike (East-West or dip direction traverse)

The 2D subsurface resistivity model (Figure 21) reveals very low resistivity (2.0 - 50 Ωm) intervals at 35-50 m, 75-77 m and 88-100 m electrode spacing positions along the eastward traverse. The IP values at these positions are generally 10 - 38 ms. The combination of low resistivity with high IP at these positions indicates deposits of graphite bodies.

The bodies lie generally within 0.7 - 12.0 m depth interval. The comparatively high resistivity (200 - 400 Ωm) and low IP (0.3 - 3.0 ms) intervals that separate the graphite bodies are inferred to be quartzite bodies. This inference is in agreement with intercalations of graphite and quartzite bodies along dip traverse (East-West direction) observed on the surface, as shown in Figure 23.

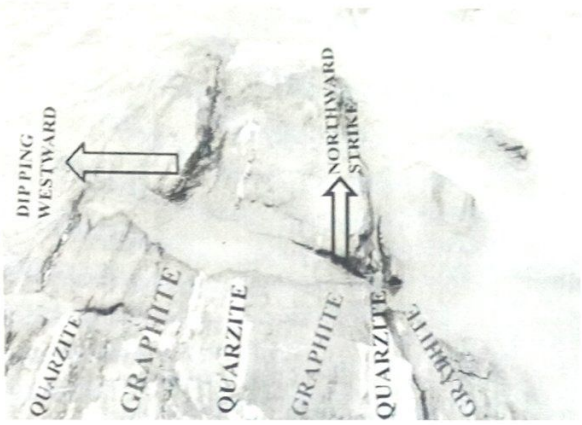

Figure 23. Intercalations of graphite and quartzite bodies along outcrop dip direction (6°15'46.08"E, 10°11'36.62 ' 'N)

Figures 24 and 25 are respectively 2D subsurface resistivity and IP models along outcrop dip traverse that cuts through the location with coordinates 6°15'43.27"E, 10°11'44.35 ' 'N.

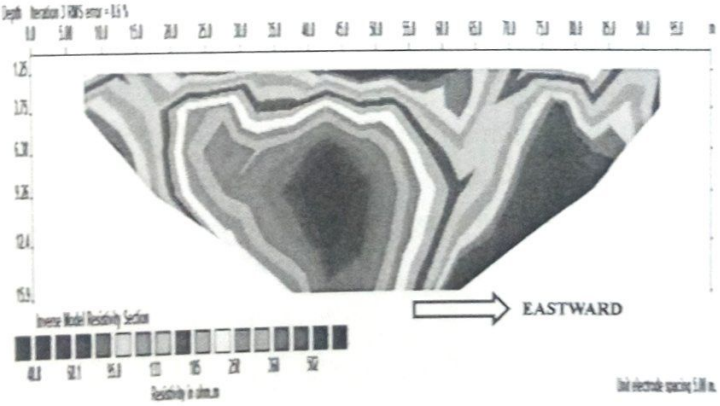

Figure 24. 2D subsurface resistivity model along outcrop dip traverse (East-West direction) through location 6°15'43.27"E; 10°11'44.35"N

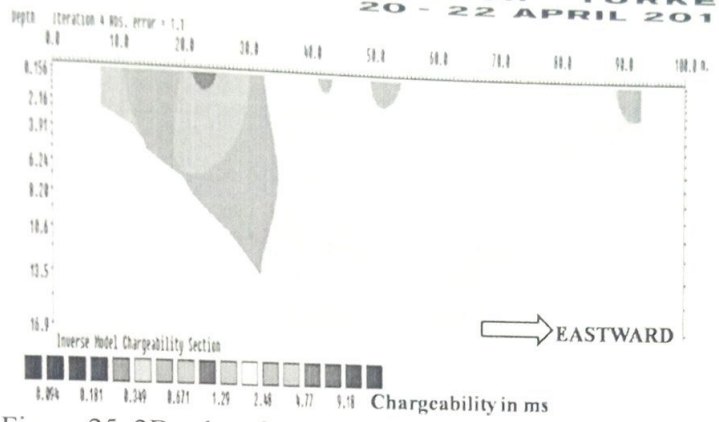

Figure 25. 2D subsurface IP model along outcrop dip traverse (East-West direction) through location 6°15'43.27"E; 10°11'44.35"N

The subsurface resistivity (Figure 24) generally ranges from about 40 - 100 Ωm along the entire traverse within 1.5 to 6.0 m depth interval. Towards the eastern end of the traverse, the resistivity is consistently lower than 95 Ωm within 3.8 to 15.9 m depth interval. This indicates that the graphite body exists throughout the traverse. The IP values (Figure 25) range from 2.0 to 9.0 ms along the traverse, thus supporting the existence of subsurface graphite body.

Figure 26 shows the delineated graphite deposit within the other rock units. This occupies an estimated surface area of 1470509.0 m^2, which multiplies with its average thickness of 10.0 m to give an estimated gross volume of 14705090.0 m^3 graphite deposit.

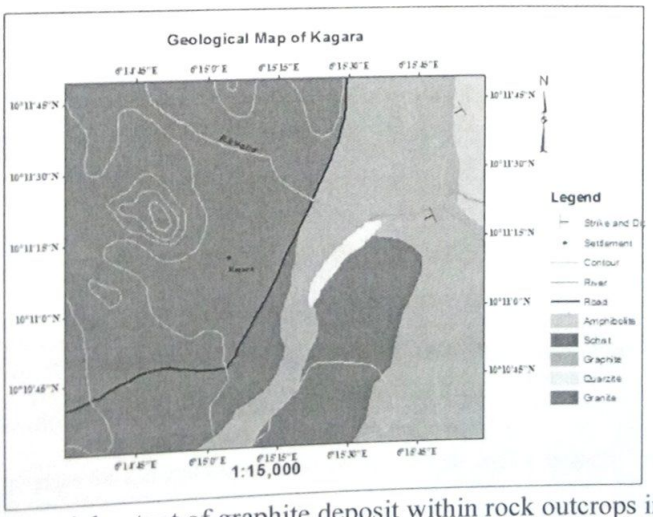

Figure 26. Spatial extent of graphite deposit within rock outcrops in Kagara

Results and Suggestions

The combination of lithologic mapping with 1D geoelectric sounding and geoelectric tomography has enabled the characterization, spatial delineation and estimation of the gross volume of graphite deposit in Kagara. The subsurface deposit was identified by combination of 2 – 100 Ωm resistivity with 2 - 100 ms IP and negative SP anomaly. The deposit exists within 0.7 - 12 m depth interval, and has an average thickness of about 10.0 m. It occupies a spatial extent of about 1470509.0 m^2 and constitutes a gross volume of about 14705090.0 m^3. The deposit appears to exist as a series of sheet-like bodies interlaid with quarzites.
The development of this deposit and other graphite deposits in Nigeria will generate employments and additional revenue in the country.

References

Ajibade, A. C., Anyanwu, N. P. C., Okoro, A. U., and Nwajide C. S., 2008. The Geology of Minna area, Bulletin 43 of Nigerian Geological Survey Agency.

Anthony, W. Bideaux, R.A., Bladh, K.W. and Nichols, M.C., 2003. Handbook of mineralogy (1):elements, sulphides,sulfosalts. Mineral Data Publishing, Tusco, Arizona.

Chernicoff, S. and Whitney, D., 2007. Geology: an introduction to physical geology, 4th edition, Pearson Education.

Dickson, J.S., 2014. Talga eyes graphene potential. Industrial minerals, 567: 35-36.

Gandhi, S.N. and Sarkar, B.C., 2016. Essential of mineral exploration and evaluation, 1st edition, Elsievier.

Kearey, P., Brooks, M. and Hill, I., 2002. An Introduction to Geophysical Exploration, Blackwell Scientific, Oxford, UK.

Meunier, E.(2015). Exploring for Graphite Using a New Ground Based Time Domain Electromagnetic System, Carleton University, M.Sc Thesis, Canada.

Milsom, J., 2003. Field Geophysics, 3rd Edition, John Wiley and Sons, UK.

Reynolds, J.M., 2011. An Introduction to Applied and Environmental Geophysics, 2nd edition, Wiley-Blackwell, Oxford.

Robinson, G.R.,Jr., Hammerstrom, J.M. and Olson, D.W. , 2017. Graphite. In: Schulz, K.J., DeYoung, J.H., Seal, R.P. and Bradley, D.C. (eds.) Critical mineral resources of the United States- Graphite . US geological survey professional paper 1802, pJ1-J24. https://doi org/10.3133/p1802J

Scott, W.J., 2014. Geophysics for Mineral Exploration, Newfoundland and Labrador Department of Natural Resources.

Shaw, S., 2013. Graphite demand and growth: the future of lithium-ion batteries in EVs and HEVs, Proceedings of 37th ECGA General Assembly.

Simandl, G.J., Pardon, S and Akam, C., 2015. Graphite deposit types, their origin and economic significance. In : Simandl, G.J. and Nextz, M. (eds.) Symposium on strategic and critical mineral proceeding, November 13-14, Victoria, British Colombia British Colombia Geological Survey paper 2015-3, p163 - 171.

Wissler, M.,2006. Graphite and carbon powder for electrochemical applications. Journal of power sources ,156: 142-150.

Yoo, H.D., Markevich, E., Salitra, G., Sharon, D. and Aurbach, D (2014)Matrials today, 17(3):110-120.